

# Journal of Materials Chemistry A

Accepted Manuscript



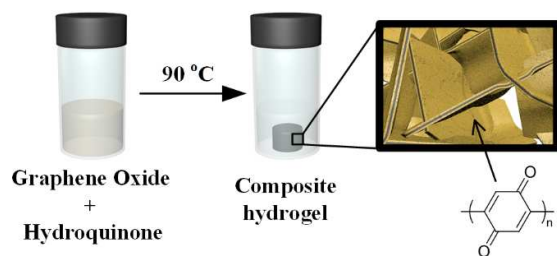
This is an *Accepted Manuscript*, which has been through the Royal Society of Chemistry peer review process and has been accepted for publication.

*Accepted Manuscripts* are published online shortly after acceptance, before technical editing, formatting and proof reading. Using this free service, authors can make their results available to the community, in citable form, before we publish the edited article. We will replace this *Accepted Manuscript* with the edited and formatted *Advance Article* as soon as it is available.

You can find more information about *Accepted Manuscripts* in the [Information for Authors](#).

Please note that technical editing may introduce minor changes to the text and/or graphics, which may alter content. The journal's standard [Terms & Conditions](#) and the [Ethical guidelines](#) still apply. In no event shall the Royal Society of Chemistry be held responsible for any errors or omissions in this *Accepted Manuscript* or any consequences arising from the use of any information it contains.

## TOC



Polyhydroquinone-graphene hydrogel composites were prepared *via* one-step reaction, and showed high specific capacitance and rate performance as the electrode material for supercapacitor.



Journal Name

ARTICLE

## One-step Synthesis of Polyhydroquinone-Graphene Hydrogel Composites for High Performance Supercapacitors†

Libin Chen, Jifeng Wu, Aijuan Zhang, Anan Zhou, Zhifeng Huang, Hua Bai\* and Lei Li\*

Received 00th January 20xx,  
Accepted 00th January 20xx

DOI: 10.1039/x0xx00000x

www.rsc.org/

Electroactive polymers constitute an important class of electrode materials of supercapacitors based on pseudocapacitance. However, it is difficult to utilize the lowly-conductive electroactive polymers in supercapacitors, although these polymers may have large theoretic specific capacitance. In this article, we designed and prepared a novel type of electrode material, with a unique structure of a lowly-conductive electroactive polyhydroquinone (PHQ) coated on the highly-conductive three-dimensional (3D) porous graphene hydrogel (GHG). The PHQ-GHG composites were prepared *via* one-step reaction between graphene oxide and hydroquinone under mild conditions. Because PHQ has large theoretic specific capacitance, and GHG possesses 3D porous structure, large specific surface area and high electric conductivity, the composites showed high specific capacitance of 490 F g<sup>-1</sup> at a current density of 24 A g<sup>-1</sup>, as well as excellent rate performance and cycling stability. These results demonstrate that PHQ-GHG composites are promising electrode materials for supercapacitors, and the method developed in this paper paves a new way to utilizing those electroactive polymers of low electric conductivities in supercapacitors.

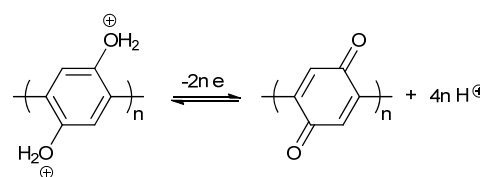
### Introduction

Electroactive polymers as electrode materials for supercapacitors have received great attention because of their large pseudocapacitance, flexible and light nature, and easy preparation.<sup>1</sup> In the last decades, a great number of supercapacitors have been fabricated based on conducting polymers (CPs), which are the most-widely used class of electroactive polymers and can provide pseudocapacitance through doping/dedoping process.<sup>2,3</sup> For electroactive polymers, the theoretic specific capacitance ( $C_T$ ) can be predicted by the following equation:<sup>4</sup>

$$C_T = \frac{nF}{\Delta E M} \quad (1)$$

where  $n$  is the average number of electrons transferred during redox reaction per repeating unit,  $F$  is the Faraday constant,  $M$  is the molecular mass of the monomer unit in the polymer, and  $\Delta E$  is the potential range in which the redox reaction occurs. So polymers with large  $n$  values are expected to have high specific capacitance. However, the values of  $n$  for CPs are strongly limited by the way in which these polymers store charges. Usually, charges are stored in CPs as polarons or bipolarons, which are particle-like structure units carrying one or two unit charges, respectively. Both polaron and bipolaron

extend on several repeating units, thus the value of  $n$  is far smaller than 1. For example, in the heavily doped polypyrrole (PPy), one bipolaron may locate on six repeating units, corresponding to a  $n$  value of 0.33.<sup>4</sup> Therefore, CT of PPy is calculated to be 1243 F g<sup>-1</sup> on the assumption that  $\Delta E$  is 0.4 V. As for polyaniline (PAni), another widely-used CP in supercapacitors, although large  $n$  value of 1 can be achieved, the CT value is calculated to be only 964 F g<sup>-1</sup>, even smaller than that of PPy, due to the larger  $\Delta E$  (~1.1 V).<sup>4</sup> Therefore, to further increase the CT of electroactive polymers, we need to design new polymers with better mechanism of charge storage, rather than storing charges with polarons or bipolarons.



Scheme 1 Structure and reversible redox reaction of PHQ in acidic aqueous solution.

Polyhydroquinone (PHQ) is an electroactive polymer which can be synthesized by oxidative polymerization of hydroquinone (HQ) and has been investigated as a suitable material for electrode modification layer. Although PHQ has a conjugated backbone, its typical electrode processes are different from the conventional CPs, due to the phenolic hydroxyl groups attaching on the backbone. The overall electrode reaction of PHQ consists of a two-electron transfer and a four-proton addition-elimination reaction, as shown in Scheme 1.<sup>5</sup> Thus the value of  $n$  for PHQ is 2, larger than those

College of Materials, Xiamen University, Xiamen, 361005, P. R. China. E-mail: baihua@xmu.edu.cn; lilei@xmu.edu.cn Address here.

† Electronic Supplementary Information (ESI) available: XPS of PHQ-GHG, possible mechanism of the reaction between PHQ and GO, GCD curves of pure PHQ electrode. See DOI: 10.1039/x0xx00000x

of CPs. As a result, the  $C_T$  value is determined to be  $3034 \text{ F g}^{-1}$ , with  $M = 106$  and  $\Delta E = 0.6 \text{ V}$ . Such a high  $C_T$  value makes PHQ an attractive candidate for electrode materials in supercapacitor. Unfortunately, the conductivity of PHQ is only  $10^{-7} \text{ S cm}^{-1}$ ,<sup>5</sup> which is much smaller than those of the doped CPs by eight orders of magnitude (the typical conductivity of CPs: PANi,  $10^1 \text{ S cm}^{-1}$ ;<sup>6</sup> PPy,  $10^1 \text{ S cm}^{-1}$ ;<sup>7</sup> polythiophene,  $10^0 \sim 10^2 \text{ S cm}^{-1}$ ).<sup>8</sup> Consequently, if PHQ is used as the electrode material in supercapacitors, it will induce a large inner resistance to the device, and also there will be a large part of PHQ molecules that cannot be utilized during charge/discharge, due to the huge voltage drop in the bulk PHQ electrode. Therefore, PHQ, like other lowly-conductive electroactive polymers, is an unsuitable electrode material for the supercapacitors.

In order to exploit the high specific capacitance of PHQ in supercapacitors, in this paper, we designed a novel three-dimensional (3D) porous PHQ-graphene hydrogel (PHQ-GHG) composite material. 3D porous GHG was introduced as the conductive matrix,<sup>9,10</sup> onto which PHQ layer was coated uniformly. Such a structure could facilitate the electron transfer between PHQ and the current collectors. Furthermore, the interconnected pores in the PHQ-GHG also allowed PHQ to be exposed to the electrolyte and provide open channels for unobstructed transport of the electrolyte. In order to synthesize the PHQ-GHG composites, we further devised a one-step reaction, in which graphene oxide (GO) was employed as the precursor for GHG and the oxidant for the polymerization of HQ. During the reaction, GO was reduced by HQ and self-assembled, yielding GHG, while HQ itself was converted into PHQ, and deposited onto the skeleton of GHG.

As a free-standing hydrogel, the PHQ-GHG composites could be used as the electrode of supercapacitors without any additions. In this paper we will demonstrate that the PHQ-GHG composite materials have high specific capacitance provided by the PHQ component, and good rate performance owing to their optimized structure. Also, the method of incorporating GHG to promote the performance of PHQ may guide us how to utilize other lowly-conductive electroactive polymers in supercapacitors.

## Results and discussion

The typical PHQ-GHG composites were easily prepared by heating GO solution containing a certain amount of HQ at  $90^\circ\text{C}$  for 24 h. The composites prepared with 5 mg, 10 mg, 30 mg, 60 mg, 80 mg HQ are named PHQ-GHG-5, PHQ-GHG-10, PHQ-GHG-30, PHQ-GHG-60 and PHQ-GHG-80, respectively. The as-prepared PHQ-GHG composite was black monolith, as shown in Fig. 1A. The preparation of PHQ-GHG composites could be easily scaled up by increasing the volume of the reaction system. As depicted in Fig. 1B, a large PHQ-GHG composite of  $\sim 16 \text{ cm}^3$  was prepared. The structure of the composite was investigated by scanning electron microscopy (SEM, Fig. 1C and D). A 3D network consisting of two-dimensional (2D) sheets is found in SEM images, and this is the typical structure of graphene-based hydrogels.<sup>11,12</sup> As demonstrated in the earlier reports, GHG could be obtained by reducing concentrated GO dispersion.<sup>11-15</sup> During the reduction, GO sheets become less hydrophilic and consequently aggregate,

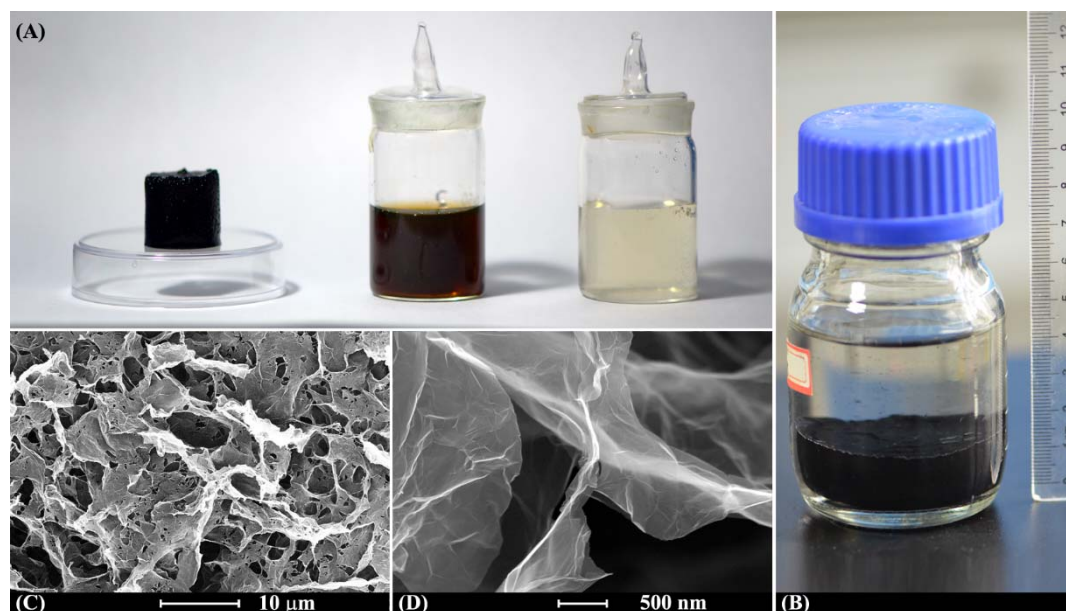


**Fig. 1** (A) Hydrothermal products of different solutions: left, GO solutions containing HQ; middle, GO solution; right, HQ solutions. (B) Large-scale product of PHQ-GHG-60 (C) (D) SEM images of PHQ-GHG-60.

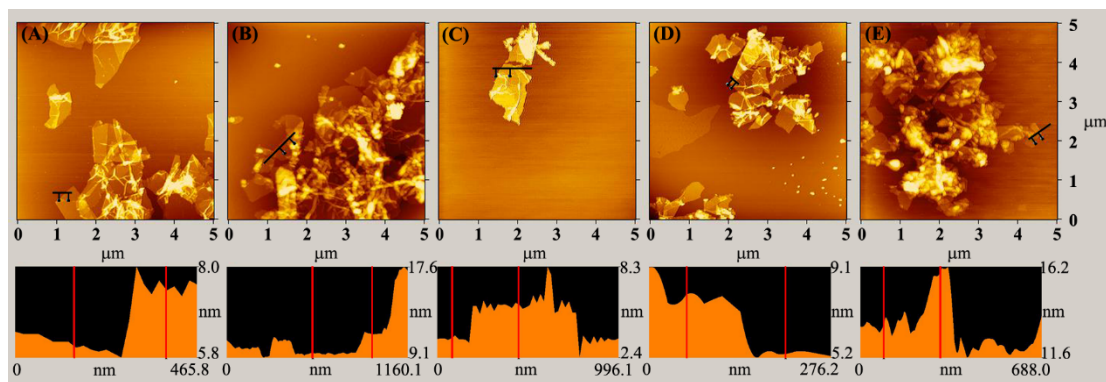


Fig. 2 AFM images of exfoliated PHQ-GHG composites. From (A) to (E): PHQ-GHG-5, -10, -30, -60, -80.

yielding 3D network. In our experiments, HQ was used as the reductant to reduce GO and promote the formation of GHG. The reduction of GO is confirmed by XPS analysis and conductivity measurement. In the XPS shown in Fig. S1, the peaks associated with oxidized carbon species become much weaker after reduction, showing that the oxygen-containing groups were removed. The electric conductivity of PHQ-GHG-60 was measured to be  $1.32 \text{ S cm}^{-1}$ , much higher than that of pure PHQ and GO, and similar to that of other chemically converted graphene (CCG),<sup>16,17</sup> further confirming the reduction of GO. The high conductivity of PHQ-GHG composites is important when they are used as electrodes. The role of HQ as the reductant in the formation of hydrogels is verified by the control experiments. As shown in Fig. 1A, no hydrogel or precipitation was found after GO solution was heated at  $90 \text{ }^\circ\text{C}$  for 24 h, revealing that GO cannot be thermally reduced at this temperature. Also pure HQ solution was not able to generate hydrogel at the same reaction condition (Fig. 1A right). Therefore, it is safe to conclude that the hydrogels resulted from the reduction of GO by HQ.

GHGs have been prepared by chemically reducing GO dispersion with various reductants, but very few attentions have been paid to the oxidation product of the reductant. In order to investigate the composition of the produced composites, we tried to separate the possible oxidation product from the composites. It was found that some yellow substance could be extracted from the PHQ-GHG composites by ethanol and other polar organic solvents. Such substance is insoluble in water, because the PHQ-GHG composites have been dialyzed in water before the extraction. Since GO, HQ and BQ are all soluble or slightly soluble in water, the extract should be the oxidation product of HQ. However, even in the magnified SEM image (Fig. 1D), no obvious particle or aggregate was found, thus we used atomic force microscopy (AFM) to further characterize the composites. Fig. 2 shows the AFM images of the 2D nanosheets in PHQ-GHGs. The thicknesses of the nanosheets are  $1.4 \sim 2.5 \text{ nm}$ , larger than that of CCG sheets prepared by chemically reducing GO ( $\sim 1 \text{ nm}$ ).<sup>18</sup> This suggests that the nanosheets in the PHQ-GHG composites are modified by a thin layer of other substance.

Therefore, we believed that the oxidation product of HQ was deposited on the surface of CCG sheets in the composites.

In order to confirm the composition of the composites, Fourier transform infrared (FT-IR) and ultraviolet-visible (UV-Vis) spectra of the extract were measured and compared with those of HQ. As depicted in Fig. 3A, the UV-Vis spectrum of HQ shows a sharp absorbance peak at  $288 \text{ nm}$  with the onset at  $315 \text{ nm}$ , corresponding to the  $\pi\text{-}\pi^*$  transition of electron in benzene ring conjugated with hydroxide group. Meanwhile, the spectrum of the extract has distinct features. No well-defined absorbance peak is found in the spectrum, and the onset wavelength of the spectrum red-shifts to  $650 \text{ nm}$ , much longer than that of HQ. Such UV-Vis spectrum agrees with that of PHQ prepared with other methods.<sup>19,20</sup> The red-shift of the

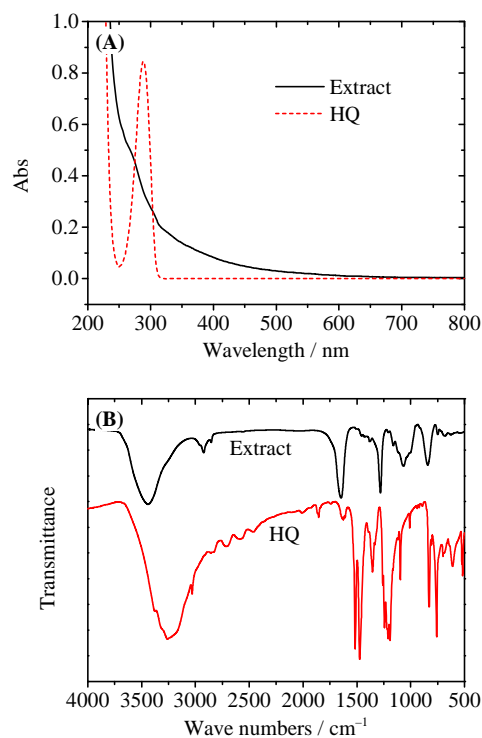


Fig. 3 (A) The UV-Vis spectrum of ethanol extract of PHQ-GHG and HQ. (B) The FT-IR spectra of the extract from PHQ-GHG and HQ.

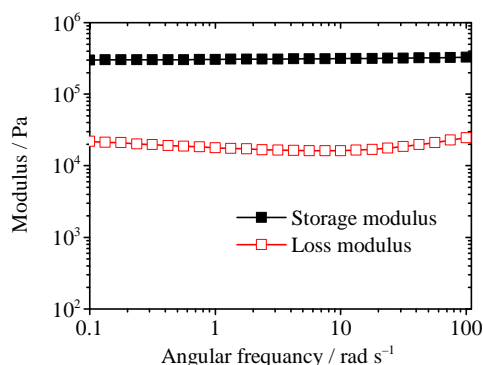


Fig. 4 Rheological behaviors of the PHQ-GHG-60.

UV-Vis spectrum indicates that the conjugate length of the extract is larger than that of HQ. Fig. 3B represents the FT-IR spectra of HQ and the extract. The FT-IR spectrum of the extract is quite different from that of HQ, but similar with that of PHQ reported in the literatures.<sup>19,20</sup> The bands in the spectrum can be assigned to the main functional groups in PHQ. The broad band at  $3500\text{ cm}^{-1}$  is attributed to the stretching of O-H in hydroxide or water. The strong band at  $1651\text{ cm}^{-1}$  is assigned to the stretching of C=O. This band is much stronger in the extract compared with that in HQ, because phenolic hydroxyls in PHQ were oxidized by GO, producing quinone structures. Moreover, bands at  $1194\text{ cm}^{-1}$  and  $756\text{ cm}^{-1}$  are associated with C-O stretching and C-H

bending, respectively. Therefore, although the detailed mechanism of the reaction between HQ and GO is unknown currently (a possible reaction mechanism was shown in Scheme S1<sup>†</sup>), from the spectral data, it is confirmed that the oxidation product of HQ is PHQ.

The mechanical property of the PHQ-GHG composite was studied by the rheological test. In Fig. 4, the storage modulus ( $G'$ ) and loss modulus ( $G''$ ) of the PHQ-GHG-60 monolith are plotted as a function of angular frequency. It can be found that  $G'$  is independent on frequency, whereas  $G''$  increases slightly with the frequency. These are the characteristic rheological behavior of gels.<sup>11,21</sup> The  $G'$  values are larger than  $10^5\text{ Pa}$ , comparable with other graphene based hydrogels.<sup>11,22,23</sup> Besides, the  $G'$  values are always one order of magnitude higher than the  $G''$  values over the experimental frequency range ( $0.1 \sim 100\text{ rad}\cdot\text{s}^{-1}$ ), indicating that elastic response of the PHQ-GHG composite is predominant, and the composite is a strong hydrogel.<sup>11</sup> The good mechanical properties allow the composite to be tailored into designed shape, and directly used as electrodes in supercapacitor devices without any additive.

The electrochemical properties of PHQ-GHG composites were first investigated in three-electrode system. As shown in Fig. 5A, a pair of redox wave around  $0.4\text{ V}$  vs. SCE are found in every CV curve, and can be attributed to the redox reaction of PHQ illustrated in Scheme 1.<sup>7,24</sup> The peak current density of the CV curve can be used to estimate the content of PHQ in the composites. As the feeding amount of HQ increased from 5

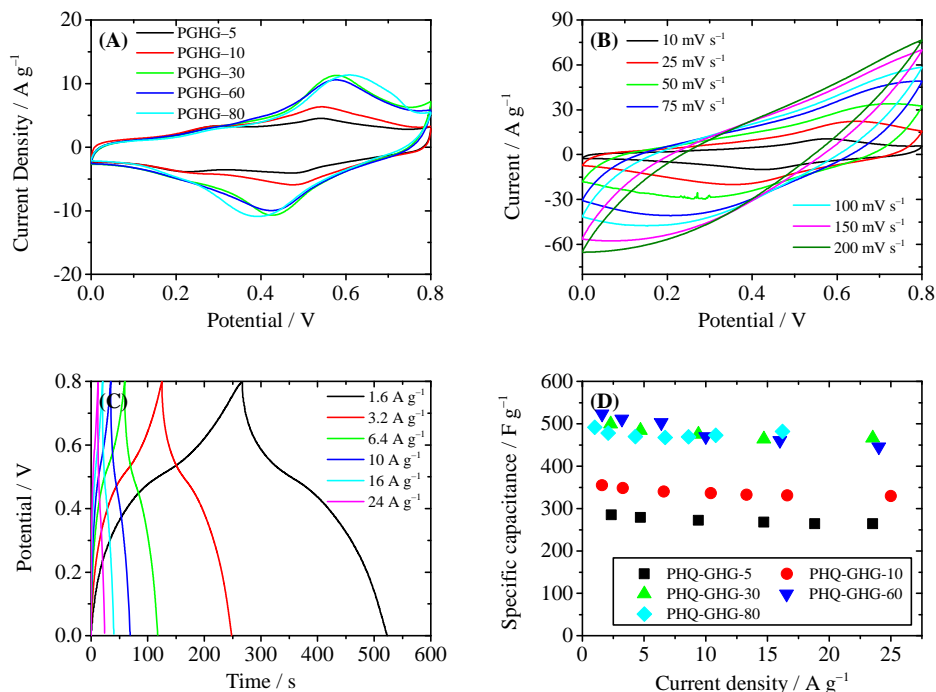
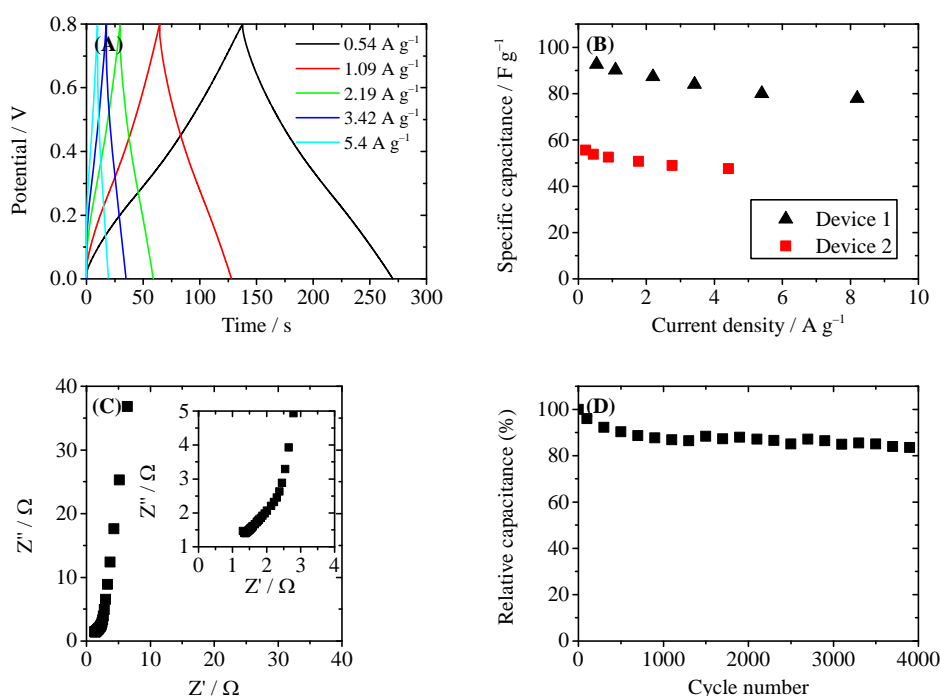


Fig. 5 Electrochemical properties of PHQ-GHG composites. (A) CV curves of different PHQ-GHG composites at the scan rate of  $10\text{ mV s}^{-1}$ . (B) CV curves of PHQ-GHG-60 at the scan rate ranging from  $10$  to  $200\text{ mV s}^{-1}$ . (C) GCD curves of PHQ-GHG-60 at the different current densities. (D) The specific capacitance of the composites at the different current densities calculated from the GCD curves.



**Fig. 6** Supercapacitance performance of the asymmetric device with PHQ-GHG-60 as the anode and GHG as the cathode (Device 1). (A) The GCD curves of Device 1 at the different current densities. (B) The specific capacitances of Device 1 and Device 2 (symmetry device with GHG as the both electrodes). (C) Electrochemical impedance spectroscopy of Device 1. Inset shows the magnified high-frequency regions. (D) The cycling stability of Device 1.

mg to 30 mg, the peak current density of anodic wave grew from 4.5 to 11.4  $\text{A g}^{-1}$ , indicating the increase in the content of PHQ in the composites. However, further increasing the feeding amount of HQ to 80 mg did not lead to larger peak current density. This suggests that excessive HQ cannot yield more PHQ in the composites. In fact, the content of PHQ in the composite is decided by the amount of both GO and HQ in the reaction system. The polymerization of HQ will stop when GO is exhausted completely. In our experiments, 30 mg HQ are sufficient to reduce all the GO in the solution, thus further increasing the feeding amount of HQ cannot produce more PHQ in the composite. This also confirms that GO is the oxidant for the polymerization of HQ. Besides, in all the CV curves, there are another pair of redox wave around 0.2 V. These waves are independent on the feeding amount of HQ, thus can be assigned to the redox reaction of the oxygen-containing groups on the CCG sheets.<sup>22,25</sup>

The CV curves of PHQ-GHG-60 at different scan rate were measured. As illustrated in Fig. 5B, at low scan rate, the potential separation between the anodic and cathode peak is small, and with the increase in the scan rate, the separation gradually became larger. This is the characteristic of quasi-reversible electrochemical reaction,<sup>26</sup> revealing the good electrochemical reversibility of the redox reaction of PHQ. The galvanostatic charge/discharge (GCD) curves of PHQ-GHG-60 were represented in Fig. 5C. There is a platform around 0.4 V in the GCD curves, corresponding to the redox wave around 0.4 V in the CV curves. The specific capacitances of these PHQ-GHG composites were calculated from GCD curves. As shown in Fig. 5D, the effect of the feeding amount of HQ on the

specific capacitance of PHQ-GHG composites agrees well with the result of CV curves. When the feeding amount of HQ was increased from 5 to 30 mg, the specific capacitances of PHQ-GHG composites rose from 290  $\text{F g}^{-1}$  to 500  $\text{F g}^{-1}$  (at the current density of approximately 2  $\text{A g}^{-1}$ ). Further increasing the feeding amount of HQ did not lead to higher specific capacitance. The specific capacitance values of these composites are much larger than that of pure GHG ( $\sim 220 \text{ F g}^{-1}$ ),<sup>22,25,27</sup> owing to the contribution of the pseudocapacitance provided by PHQ. Moreover, all the composites show good rate performance. For example, the specific capacitance of PHQ-GHG-30 is 500  $\text{F g}^{-1}$  at the current density of 2  $\text{A g}^{-1}$ , and this value only slightly decreases to 490  $\text{F g}^{-1}$  when the current density rises to 24  $\text{A g}^{-1}$ . The above experimental results suggest that PHQ-GHG composites are promising electrode materials for supercapacitor.

As we known, PHG is an unsuitable choice for the electrode materials. In fact, the specific capacitance of PHG is measured to be only 0.35  $\text{F g}^{-1}$  at a current density of 0.5  $\text{A g}^{-1}$  (Fig. S2). This is because the conductivity of PHG is very low, and consequently only the small layer of PHG near the current collector can react during the charge/discharge process. However, in the PHQ-GHG composites, PHQ is coated onto the GHG skeleton, which serves as a 3D pathway for the electrons to transfer between the current collector and PHQ.<sup>28-31</sup> The PHQ layer on GHG skeleton is very thin, thus all the PHQ molecules can be utilized during the charge/discharge process. The 3D porous structure of the composites is very important for the high performance. On one hand, the interconnected channels in the 3D porous composites allow the electrolyte to

diffuse rapidly, ensuring the high rate performance of the composites. On the other hand, the 3D porous composite has a large specific surface area ( $540 \text{ m}^2 \text{ g}^{-1}$  measured by methylene blue adsorption technique),<sup>31,32</sup> which contributes a large double layer capacitance to the total capacitance. Also larger surface area enable us to load more PHQ, even the thickness of the PHQ layer is small. As a result, the PHQ-GHG composites show both high specific capacitance and good rate performance.

We further setup an asymmetric capacitor with PHQ-GHG-60 as the anode and GHG as the cathode (Device 1). Considering that the specific capacitance of PHQ-GHG-60 is larger than that of GHG, we used a lighter anode and a heavier cathode to achieve balanced capacitances of the two electrodes. In Device 1, the areal mass loading of anode and cathode were  $3.9$  and  $7.7 \text{ mg cm}^{-2}$ , respectively. The GCD curves of Device 1 at different current densities shown in Fig. 6B are deformed triangles, the characteristic GCD curves of supercapacitors. The capacitance of PHQ-GHG anode is larger than that of GHG cathode, thus the GCD curve of the device resembles that of the cathode in shape, which is a triangle.<sup>33</sup> According to Eqn. 2 and 3, the specific capacitances of Device 1 were calculated to be  $92.6 \text{ F g}^{-1}$  at  $0.54 \text{ A g}^{-1}$  and  $77.9 \text{ F g}^{-1}$  at  $8.2 \text{ A g}^{-1}$ , as shown in Fig. 6C. For a comparison, a symmetry device with two GHG electrodes was also fabricated and tested (Device 2). The specific capacitances of Device 2 were  $53.7 \text{ F g}^{-1}$  at  $0.44 \text{ A g}^{-1}$  and  $47.5 \text{ F g}^{-1}$  at  $4.4 \text{ A g}^{-1}$ . Therefore, PHQ-GHG anode significantly improved the specific capacitance of the device. The rate performance of Device 1 was further studied by electrochemical impedance spectroscopy. Fig. 6C depicts the Nyquist plot of Device 1. It starts with a  $45^\circ$  region, which is attributed to the porous structure of the PHQ-GHG and GHG electrodes. At low frequencies, the straight line is nearly perpendicular to the real axis, indicating the purely capacitive behavior of the device. We also measured the cycling stability of Device 1. Fig. 6D represents the change of specific capacitance of Device 1 during cycling GCD at a constant current density of  $3.4 \text{ A g}^{-1}$ . The specific capacitance of Device 1 remains 83% after 4000 cycles. The good chemical stability of both PHQ and CCG endues the composites with high cycling performance, which is important for practical application.

## Conclusion

In summary, in this paper we designed and prepared novel PHQ-GHG composites, which were used as the electrode materials for the high-performance supercapacitor. The PHQ-GHG composites were synthesized *via* a simple one-step reaction, in which GO was reduced by HQ and self-assembled into 3D GHG, while HQ was oxidized and polymerized, producing a thin layer of PHQ deposited on the GHG skeleton. The PHQ-GHG composites have 3D porous structure, which facilitates the diffusion of the electrolytes, and the high electric conductivity of GHG skeleton allows the electrons to transfer freely between PHQ and the current collector. In this way, the high specific capacitance of PHQ is successfully

exploited. The specific capacitance of the PHQ-GHG composite was measured to be  $490 \text{ F g}^{-1}$  when the current density was  $24 \text{ A g}^{-1}$ . An asymmetric capacitor device with PHQ-GHG as the anode and GHG as the cathode was also fabricated, and showed a high specific capacitance of  $77.9 \text{ F g}^{-1}$  at  $8.2 \text{ A g}^{-1}$ , as well as good cycling stability. These results indicate that the PHQ-GHG composites are promising electrode materials for supercapacitor. Besides, we also demonstrated that GHG, with high surface area and good electric conductivity, is an excellent matrix for constructing composite electrode and supporting the lowly-conductive electroactive materials. We believe this work can further inspire the design of other novel high-performance electrode materials for the supercapacitors.

## Experimental

### Materials

HQ (analytically pure) and sulfuric acid ( $\text{H}_2\text{SO}_4$ , 98%) were purchased from Sinopharm Chemical Reagent Co., Ltd, and used as received. GO was prepared by oxidation of natural graphite powder (325 mesh, Qingdao Huatai lubricant sealing S&T Co. Ltd.) according to a modified Hummers' method.<sup>34</sup>

### Preparation of PHQ-GHG and GHG

The PHQ-GHG composites were prepared by heating 5 mL GO aqueous solution ( $2 \text{ mg mL}^{-1}$ ) containing different amount of HQ at  $90^\circ \text{C}$  for 24 h. After reaction, the as-produced composites were dialyzed in pure water for 24 h to remove any impurities. GHG was prepared following the reported procedure.<sup>11</sup> 10 mL GO solution ( $2 \text{ mg mL}^{-1}$ ) was sealed in a Teflon-lined autoclave and heated at  $180^\circ \text{C}$  for 24 h. Then the as-prepared GHG was further reduced by hydrazine hydrate (50%) at  $95^\circ \text{C}$  for 8 h.<sup>27</sup> Finally, GHG was dialyzed in pure water for 24 h.

### Electrochemical measurement

The capacitance performance of PHQ-GHG composites was investigated in two-electrode and three-electrode systems. In all the electrochemical tests,  $4 \text{ M H}_2\text{SO}_4$  was used as the electrolyte. For the two-electrode test, a model supercapacitor device was assembled, with two platinum foils as the current collectors, and a piece of PHQ-GHG and GHG as the anode and the cathode, respectively. The areal mass loading of the electrode was  $4.0 \sim 5.5 \text{ mg cm}^{-2}$  (efficient electrode area:  $0.646 \text{ cm}^2$ ), unless specified otherwise. Before the setup of the device, the PHQ-GHG and GHG were immersed in the electrolyte overnight to exchange their interior water with the electrolyte. A silicon rubber gasket was sandwiched between the platinum foils to seal the device, and the device was hold together by a clamp. The symmetry device was assembled with the same method except that both electrodes were GHG. The specific capacitance of the device was measured by galvanostatic charge/discharge (GCD) method and calculated according to the following equation:

$$C_s = \frac{Jt}{V - IR}, \quad (2)$$

$$\text{and } J = \frac{I}{m_A + m_C}, \quad (3)$$

where  $I$  is the current applied on the device,  $t$  is the discharge time,  $m_A$  and  $m_C$  is the mass of the anode and the cathode,  $V$  is the highest voltage in the GCD curves, and  $IR$  represents the voltage drop at the beginning of the discharge process, caused by internal resistance of the device.

To test the electrochemical performance of PHQ-GHG composites in a three-electrode system, the above two-electrode device was immersed into an electrochemical cell filled with 4 M H<sub>2</sub>SO<sub>4</sub>. Two channels were cut on the silicon rubber gasket, to ensure the connectivity of the electrolyte in the device and the cell. The PHQ-GHG electrode was used as the working electrode and the GHG electrode as the counter electrode. A saturated calomel electrode (SCE) was employed as the reference electrode. The specific capacitances of PHQ-GHG composites were calculated according to the following equation:

$$C_s = \frac{Jt}{\Delta V - IR}, \quad (4)$$

$$\text{and } J = \frac{I}{m}, \quad (5)$$

where  $\Delta V$  is potential range of the GCD process, and  $m$  is the mass of the PHQ-GHG electrode;  $I$ ,  $t$  and  $IR$  have the same definitions as in Eqn. (2) and (3).

### Characterization

All the electrochemical measurements were conducted on an electrochemical workstation (CHI 660). The morphology of the composites was observed using the field emission scanning electron microscope (LEO 1530) operated at 20 kV. Atomic force microscopy images were collected on a scanning probe microscope (SPA 400, Seiko Instrument) in tapping mode. Fourier transform infrared (FT-IR) spectra were obtained on the Avatar 360 spectrometer (Thermo Nicolet), and ultraviolet-visible (UV-Vis) spectra were gained on the UV-2550 spectrometer (Shimadzu). X-ray photoelectron spectra (XPS) were collected on the PHI Quantum 2000 spectrometer using monochromatic X-rays from an Al K $\alpha$  source with a takeoff angle of 45° from the surface plane.

### Acknowledgements

This work was financially supported by the National Natural Science Foundation of China (21104041, 21444004).

### Notes and references

- 1 B. E. Conway, V. Birss, J. Wojtowicz, *J. Power Sources* **1997**, *66*, 1.
- 2 R. J. Waltman, *Can. J. Chem.* **1986**, *64*, 76.

- 3 B. K. Kuila, B. Nandan, M. Bohme, A. Janke, M. Stamm, *Chem. Commun.* **2009**, 5749.
- 4 C. Peng, D. Hu, G. Z. Chen, *Chem. Commun.* **2011**, *47*, 4105.
- 5 K. Yamamoto, T. Asada, H. Nishide, E. Tsuchida, *Bull. Chem. Soc. Jpn.* **1990**, *63*, 1211.
- 6 A. J. Epstein, *Synth. Met.* **1987**, *18*, 303.
- 7 H. C. Kang, K. E. Geckeler, *Polymer* **2000**, *41*, 6931.
- 8 Y. Furukawa, M. Akimoto, I. Harada, *Synth. Met.* **1987**, *18*, 151.
- 9 Y. Zhao, H. Bai, Y. Hu, Y. Li, L. Qu, S. Zhang, G. Q. Shi, *J. Mater. Chem.* **2011**, *21*, 13978.
- 10 Y. Zhao, J. Liu, Y. Hu, H. H. Cheng, C. G. Hu, C. C. Jiang, L. Jiang, A. Y. Cao, L. T. Qu, *Adv. Mater.* **2013**, *25*, 591.
- 11 Y. X. Xu, K. X. Sheng, C. Li, G. Q. Shi, *ACS Nano* **2010**, *4*, 4324.
- 12 C. Li, G. Q. Shi, *Adv. Mater.* **2014**, *26*, 3992.
- 13 K. W. Chen, L. B. Chen, Y. Q. Chen, H. Bai, L. Li, *J. Mater. Chem.* **2012**, *22*, 20968.
- 14 P. Chen, J.-J. Yang, S.-S. Li, Z. Wang, T.-Y. Xiao, Y.-H. Qian, S.-H. Yu, *Nano Energy* **2013**, *2*, 249.
- 15 Z. S. Wu, A. Winter, L. Chen, Y. Sun, A. Turchanin, X. Feng, K. Mullen, *Adv. Mater.* **2012**, *24*, 5130.
- 16 Y. X. Xu, H. Bai, G. W. Lu, C. Li, G. Q. Shi, *J. Am. Chem. Soc.* **2008**, *130*, 5856.
- 17 S. Park, J. An, I. Jung, R. D. Piner, S. J. An, X. Li, A. Velamakanni, R. S. Ruoff, *Nano Lett.* **2009**, *9*, 1593.
- 18 D. Li, M. B. Müller, S. Gilje, R. B. Kaner, G. G. Wallace, *Nat. Nanotechnol.* **2008**, *3*, 101.
- 19 A. Zhang, J. He, Y. Guan, Z. Li, Y. Zhang, J. X. Zhu, *Sci. China Chem.* **2012**, *55*, 830.
- 20 J. He, A. Zhang, Y. Zhang, Y. Guan, *Macromolecules* **2011**, *44*, 2245.
- 21 H. Bai, K. X. Sheng, P. F. Zhang, C. Li, G. Q. Shi, *J. Mater. Chem.* **2011**, *21*, 18653.
- 22 K. X. Sheng, Y. X. Xu, C. Li, G. Q. Shi, *New Carbon Mater.* **2011**, *26*, 9.
- 23 Z. Sui, X. Zhang, Y. Lei, Y. Luo, *Carbon* **2011**, *49*, 4314.
- 24 P. Wang, B. D. Martin, S. Parida, D. G. Rethwisch, J. S. Dordick, *J. Am. Chem. Soc.* **1995**, *117*, 12885.
- 25 Y. Chen, X. Zhang, D. Zhang, P. Yu, Y. Ma, *Carbon* **2011**, *49*, 573.
- 26 A. J. Bard, L. R. Faulkner, *Electrochemical Methods: Fundamentals and Applications*, John Wiley & Sons, New York, USA, 2001.
- 27 L. Zhang, G. Q. Shi, *J. Phys. Chem. C* **2011**, *115*, 17206.
- 28 X. Feng, Z. Yan, N. Chen, Y. Zhang, Y. Ma, X. Liu, Q. Fan, L. Wang, W. Huang, *J. Mater. Chem. A* **2013**, *1*, 12818.
- 29 G. Zhu, Z. He, J. Chen, J. Zhao, X. Feng, Y. Ma, Q. Fan, L. Wang, W. Huang, *Nanoscale* **2014**, *6*, 1079.
- 30 X. Feng, N. Chen, Y. Zhang, Z. Yan, X. Liu, Y. Ma, Q. Shen, L. Wang, W. Huang, *J. Mater. Chem. A* **2014**, *2*, 9178.
- 31 X. Feng, Z. Yan, N. Chen, Y. Zhang, X. Liu, Y. Ma, X. Yang, W. Hou, *New J. Chem.* **2013**, *37*, 2203.
- 32 M. J. Mcallister, J.-L. Li, D. H. Adamson, H. C. Schniepp, A. A. Abdala, J. Liu, M. Herrera-Alonso, D. L. Milius, R. Car, R. K. Prud'homme, I. A. Aksay, *Chem. Mater.* **2007**, *19*, 4396.
- 33 L. Chen, H. Bai, Z. Huang, L. Li, *Energy Environ. Sci.* **2014**, *7*, 1750.
- 34 Y. Q. Chen, K. W. Chen, H. Bai, L. Li, *J. Mater. Chem.* **2012**, *22*, 17800.